Opto-Electronics Review

journal homepage: https://journals.pan.pl/opelre

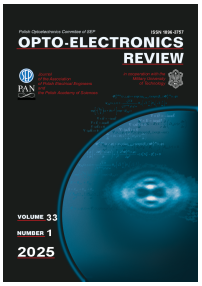

Underwater Laguerre-Gaussian beam propagation and phase compensation method

Haotian Shi[1,2], Xiaoyue Wang[3*], Yani Zuo[2], Hao Qiao[4] , Limeng Luo[4]

[1] College of Metrology Measurement and Instrument, China Jiliang University, Hangzhou 310018, China
[2] Division of Time and Frequency Metrology, National Institute of Metrology (NIM), Beijing 100029, China
[3] College of Optical and Electronic Technology, China Jiliang University, Hangzhou 310018, China
[4] Tianfu Xinglong Lake Laboratory, Chengdu 610213, China

Article info

Article history:
Received 07 Oct. 2024
Received in revised form 18 Nov. 2024
Accepted 02 Dec. 2024
Available on-line 18 Dec. 2024

Keywords:
Laguerre-Gaussian beam;
vortex beam;
underwater beam propagation;
phase twist.

Abstract

Laguerre-Gaussian (LG) beams experience phase twist after long-distance transmission, making the orbital angular momentum (OAM) indistinguishable. This phenomenon becomes more severe in water due to the higher refractive index. Based on the physical principles of LG beams, this paper derives the mathematical expression for LG beam transmission in water to address this issue. It organizes and analyses the physical significance of each term. The exponential term responsible for phase twist is separated and phase compensation is applied to the initial LG beam. Simulation results show that after transmission through water, traditional LG beams exhibit a clockwise twisted distribution of isophase lines. By applying the phase compensation method proposed in this paper, the phase of the initial LG beam is modulated and when the LG beam reaches the observation plane, the isophase lines become straight, verifying the effectiveness of the method. This compensation method holds significant value for LG beams in advanced physics research.

1. Introduction

Laguerre-Gaussian (LG) beam is a typical vortex beam with the characteristics of orbital angular momentum (OAM) and is widely used in cutting-edge research fields such as quantum technology, imaging, and communication [1–5]. The method to generate LG beams is quite simple – by modulating a Gaussian beam using a spatial light modulator or a spiral phase plate, the output beam becomes an LG beam [6–8]. LG beams possess a spiral phase distribution, carry OAM and can transmit information, making them highly significant in advanced physics research [9–11]. Since LG beams can carry more information, they have also been widely applied in underwater research [12–14].

In recent years, an extensive and deep research has been conducted on underwater LG beams. Zhang *et al*. present a method for generating LG beams for underwater optical communication systems [15]. They demonstrate the advantages of these beams over traditional methods in terms of improved transmission efficiency and reduced scattering effects. Xu *et al*. provided a theoretical framework for modelling the behaviour of LG beams in oceanic conditions, considering various environmental factors [16]. The findings assisted in predicting beam performance and optimizing underwater optical systems. Colin *et al*. evaluated the performance of LG against Bessel beams in underwater environments [17]. The findings indicated that LG beams offer superior depth penetration and focus on stability performance. Cheng *et al*. developed the analytical formulas for the OAM mode density and the OAM mode detection probability based on the Rytov approximation theory [18]. The study indicated that oceanic turbulence produced stronger effects on the LG beam than the atmosphere environment, which was of interest for the research of underwater quantum communication. Guo *et al*. established a far-field scattering electric Monte Carlo method for underwater LG beam propagation [19]. The study focused on the performance of LG beams on a larger scale and low doping concentration medium, investigating transmission, reflection, and target-free imaging in water. Zhang *et al*. proposed an underwater optical communication model with

*Corresponding author at: xywang_phy@163.com

https://doi.org/10.24425/opelre.2025.153161
1896-3757/ Association of Polish Electrical Engineers (SEP) and Polish Academic of Sciences (PAS). Published by PAS

the LG beam in absorbed and turbulent seawater [20]. The study showed that large topological charges were not conducive to high information transmission capacity and that the transmission capacity is influenced by absorption and signal wavelength. The information capacity was the highest with a topological charge of 1 and a wavelength of 410 nm. This has significant implications for guiding underwater communication using LG beams.

The traditional technique to identify the phase distribution is an interferometry method. However, for a short-distance transmission, the phase of the LG beam is clear and the OAM can be clearly identified [21–23]. The phase in the central region of the LG beam is minimally disturbed. However, after a long-distance transmission, the phase of the LG beam becomes twisted and deformed, making the OAM indistinguishable, which severely impacts quantum sensing, imaging, and communication [24–26]. Additionally, due to the higher refractive index of water, this phase twist becomes more pronounced in underwater environments [27, 28]. Therefore, there is an urgent need to study a phase compensation method for underwater LG beams.

To address this issue, this paper presents a method for compensating phase twist and investigating the transmission characteristics of LG beams in water. By applying the physical principles of LG beams, the expression for the LG beam transmission in water is derived using the initial light field and diffraction integral with the exponential term causing phase twist isolated. Phase modulation is then applied to the initial LG beam. Simulations demonstrate that the proposed underwater phase compensation method keeps the isophase lines straight after transmission, significantly improving the accuracy of OAM estimation and verifying its effectiveness. The approach can be extended to LG beams with higher or negative topological charges. Theoretically, this paper explores the transmission characteristics and phase compensation techniques for LG beams in deep seawater, offering potential value for LG beams and other vortex beams in underwater communication, imaging, and quantum sensing.

2. Theory

In this section, a theoretical analysis of the underwater LG beam is introduced. First, the underwater propagation of the LG beam is derived. Then, the underwater phase compensation method is proposed.

2.1. Underwater LG beam propagation characteristics

The LG beam is a traditional vortex beam, characterised by a hollow intensity distribution and a helical phase structure. An LG beam is generated by modulating the phase of a Gaussian beam using a spatial light modulator or a spiral phase plate. At z = 0, the expression for the LG beam is:

$$E_{z=0}(x,y,0)=E_0\left(\frac{\sqrt{x^2+y^2}}{\omega_0}\right)^l \exp\frac{-\left(x^2+y^2\right)}{\omega_0^2}\exp(il\phi), \quad (1)$$

where E_0 is the electric field coefficient, ω_0 is the radius of the Gaussian beam, l is the topological charge number.

Observing from the initial plane, for each beam element with the same phase, their traces are rays emitted from the initial point (x_0, y_0, 0). Due to diffraction law, after a propagation distance of z, the electronic field $E(x, y, z)$ in the observation plane is:

$$E(x,y,z)=-\frac{ik}{2\pi z}\exp(ikz)\iint E_{z=0}\left(x_0,y_0,0\right) \cdot\exp\left[\frac{ik}{2z}\left(x-x_0\right)^2+\left(y-y_0\right)^2+z^2\right]\mathrm{d}x_0\,\mathrm{d}y_0, \quad (2)$$

where k is the wave number. In water, $k=2\pi n_{\text{water}}/\lambda$, n_{water} is the refractive index of water.

Substitute $E_z=0$ into (2):

$$E(x,y,z)=-\frac{ikE_0}{2\pi z}\exp(ikz)\exp\left[\frac{ik}{2z}\left(x^2+y^2\right)\right]\iint\left(\frac{x_0+iy_0}{\omega_0}\right)^l \cdot\exp\left[\left(\frac{ik}{2z}-\frac{1}{\omega_0{}^2}\right)^2\left(x_0{}^2+y_0{}^2\right)-\frac{ik}{z}\left(xx_0+yy_0\right)\right]\mathrm{d}x_0\,\mathrm{d}y_0. \quad (3)$$

Let

$$\alpha=x_0+ikx/[2z(1/\omega_0{}^2-ik/2z)],$$
$$\beta=y_0+iky/[2z(1/\omega_0{}^2-ik/2z)],$$

equation (3) is transformed as:

$$E(x,y,z)=-\frac{ikE_0}{2\pi z}\exp(ikz)\exp\left[\frac{ik\left(x^2+y^2\right)}{2\omega_0^2\left(\frac{ik}{2z}-\frac{1}{\omega_0^2}\right)^2 z}\right] \iint\exp\left[-\left(\frac{ik}{2z}-\frac{1}{\omega_0^2}\right)^2\left(\alpha^2+\beta^2\right)\right] \cdot\left[\frac{\alpha+i\beta+k(y-ix)}{2\left(\frac{ik}{2z}-\frac{1}{\omega_0^2}\right)^2 z\omega_0}\right]\mathrm{d}\alpha\,\mathrm{d}\beta. \quad (4)$$

Integrating (4), the electronic field of the LG beam with the propagation distance of z is expressed as:

$$E(x,y,z)=-iE_0\left(\frac{y-ix}{\omega_0}\right)^l\left[\frac{k}{2\left(\frac{ik}{2z}-\frac{1}{\omega_0^2}\right)^2 z}\right]^{l+1} \cdot\exp\left[\frac{ik\left(x^2+y^2\right)}{2\omega_0^2\left(\frac{ik}{2z}-\frac{1}{\omega_0^2}\right)^2 z}\right]\exp(ikz). \quad (5)$$

By changing the input parameters, such as beam radius, topological charge intensity and propagation distance, the beam evolution of any beam at any position can be obtained. Rearranging (5), it can be obtained:

$$E(\mathbf{r},z)=E_0(-i)^{l+1}\left(\sqrt{1+\frac{4z^2}{k^2\omega_0^4}}\right)^l\exp(il\phi)\cdot\exp\left[-\frac{\mathbf{r}^2}{\omega_0^2\left(1+\frac{4z^2}{k^2\omega_0^4}\right)}\right]\exp\left[ikz+\frac{i\cdot 2z\mathbf{r}^2}{k\omega_0^4\left(1+\frac{4z^2}{k^2\omega_0^4}\right)}\right]. \quad (6)$$

Equation (6) is very similar in form to (1). The first exponential term contains the topological charge, representing the helical phase structure. The second exponential term indicates the isophase points are transmitted forward along the diverging rays from the initial position. The third exponential term contains the phase twist. After a long-distance transmission of the underwater LG beam, the isophase lines are no longer straight. Moreover, it can be observed that (6) contains the wavenumber parameter k which is related to the refractive index. Compared to air, water has the higher refractive index. As a result, when an LG beam is transmitted through water, it experiences a longer optical path, leading to a more severe phase twist and making the OAM difficult to distinguish. Therefore, an urgent need is to investigate a phase compensation method to correct the vortex phase of LG beams in water.

2.2. *Underwater phase compensation method*

In some underwater studies using the LG beam, such as communication, imaging, and quantum sensing, the transmission distance of the LG beam is already known. Researchers aim for the OAM to be distinguishable when the LG beam reaches a specific observation plane. To meet this requirement, for the given transmission distance Z, based on (6), a phase compensation term is added:

$$E_{\text{compensation}}(\mathbf{r},z)=E(\mathbf{r},z)\exp\left[-ikZ-\frac{i\cdot 2Z\mathbf{r}^2}{k\omega_0^4\left(1+\frac{4Z^2}{k^2\omega_0^4}\right)}\right]. \quad (7)$$

The exponential term in (7) is a phase compensation term modulated on the initial LG beam. For a certain propagation distance Z, this term compensates for the phase twist and at the end of propagation, the isophase lines change from arc curves to straight lines.

3. Results and discussions

This section primarily covers two parts: the first is the numerical calculation of the underwater LG beam propagation and the second part is the underwater phase compensation of the LG beam.

3.1. *Underwater LG beam propagation*

First, the underwater LG beam propagation based on (6) is performed. The Gaussian beam has a radius of 0.8 mm and a centre wavelength of 532 nm with a topological charge of 3. The underwater refractive index is 1.33. Figures 1(a) and (i) demonstrate the initial light intensity field and phase profile. Figure 1(e) shows the cross-section light intensity profile. After a 1 m transmission in water, the light profile, cross-section light intensity profile, and phase profile are shown in Figs. 1(b), (f), and (j). It can be observed that the light intensity profile has broadened and the phase is twisted. From Figs. 1(i) and (j), the isophase changes from straight lines to clockwise curves. For the condition of a larger topological charge of 11 and a longer propagation distance of 10 m, with other beam parameters remaining unchanged, the initial intensity profile, cross-section intensity profile, and phase profile are shown in Figs. 1(c), (g), and (k). Compared to previous calculations, for an LG beam with a larger topological charge, the dark region in the hollow part of the light field occupies a larger proportion and the phase distribution becomes more complex. After 10 m of underwater transmission, the intensity profile, cross-section intensity profile, and phase distribution are shown in Figs. 1(d), (h) and (l). In Figs. 1(c) and (d), after 10 m transmitting through water, the beam size increases due to diffraction, the dark region at the centre expands, and the light ring becomes thicker.

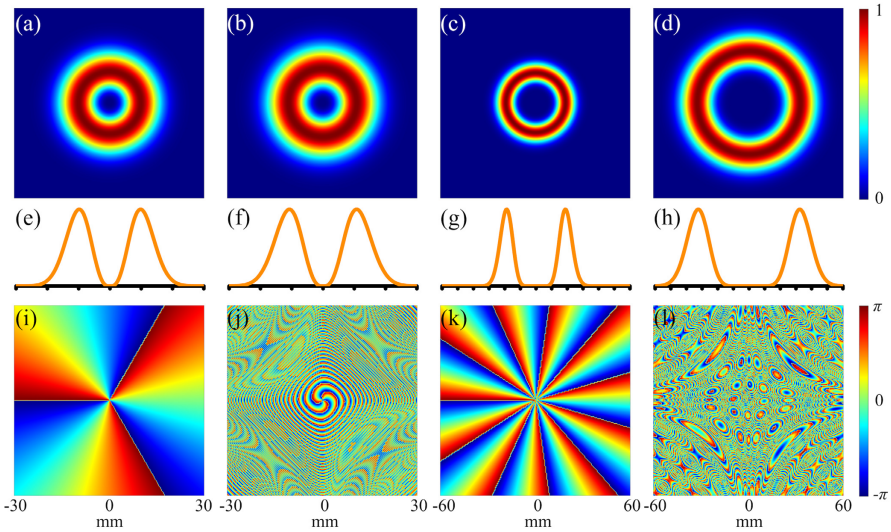

Fig. 1. Intensity profile of: (a) $l=3$, $z=0$ m; (b) $l=3$, $z=1$ m; (c) $l=11$, $z=0$ m; (d) $l=11$, $z=10$ m; cross-section intensity profile of: (e) $l=3$, $z=0$ m; (f) $l=3$, $z=1$ m; (g) $l=11$, $z=0$ m; (h) $l=11$, $z=10$ m; phase profile of: (i) $l=3$, $z=0$ m; (j) $l=3$, $z=1$ m; (k) $l=11$, $z=0$ m; (k) $l=11$, $z=10$ m.

Additionally, in the experiment, phase measurements are conducted using interference methods. The larger the dark region near the optical axis, the more difficult it is to measure the phase. Moreover, in Fig. 1(l), the phase distribution is twisted and disordered, making it completely impossible to distinguish the topological charge and OAM. Therefore, there is an urgent need for a compensation method to resolve the phase twist after a long-distance underwater transmission of LG beams.

3.2. Underwater phase compensation

Then, based on (7), a numerical simulation of underwater phase compensation is performed. The Gaussian beam has a radius of 0.8 mm and a centre wavelength of 532 nm, with a topological charge of 3. The underwater propagation distance is 1 m, with the refractive index of 1.33. The revolution of beam intensity, cross-section intensity, and phase distribution are shown in Figs. 2(a) to (e), Figs. 2(f) to (j), and Figs. 2(k) to (o). Due to the short transmission distance, the divergence of the LG beam is not significant. As shown in Fig. 2(k), by modulating the phase of the initial LG beam to create counter-clockwise isophase lines, the phase is corrected after 1 m of transmission and the isophase lines transform from curves into straight lines when reaching the target position. Figure 3 shows the underwater phase compensation method with higher topological charge and longer propagation distance. The Gaussian beam has a radius of 0.8 mm and a centre wavelength of 532 nm, with a topological charge of 11. The underwater propagation distance is 10 m, with the refractive index of 1.33. From Figs. 3(a) to (j), it can be observed that as the transmission distance increases, the size of the LG beam also increases. Additionally, the

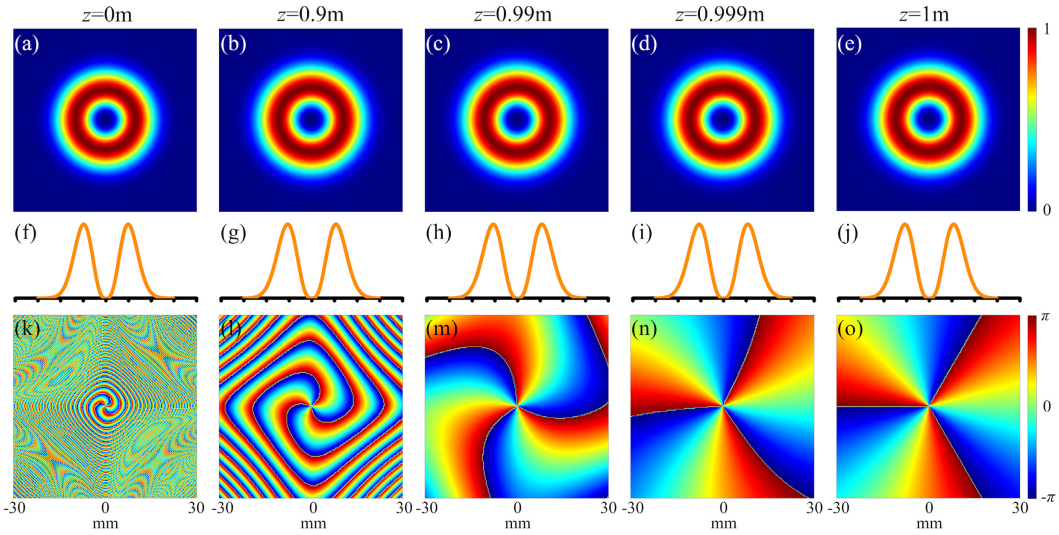

Fig. 2. Intensity profile of: (a) $l = 3$, $z = 0$ m; (b) $l = 3$, $z = 0.9$ m; (c) $l = 3$, $z = 0.99$ m; (d) $l = 3$, $z = 0.999$ m; (e) $l = 3$, $z = 1$ m; cross-section intensity profile of: (f) $l = 3$, $z = 0$ m; (g) $l = 3$, $z = 0.9$ m; (h) $l = 3$, $z = 0.99$ m; (i) $l = 3$, $z = 0.999$ m; (j) $l = 3$, $z = 1$ m; phase profile of: (k) $l = 3$, $z = 0$ m; (l) $l = 3$, $z = 0.9$ m; (m) $l = 3$, $z = 0.99$ m; (n) $l = 3$, $z = 0.999$ m; (o) $l = 3$, $z = 1$ m.

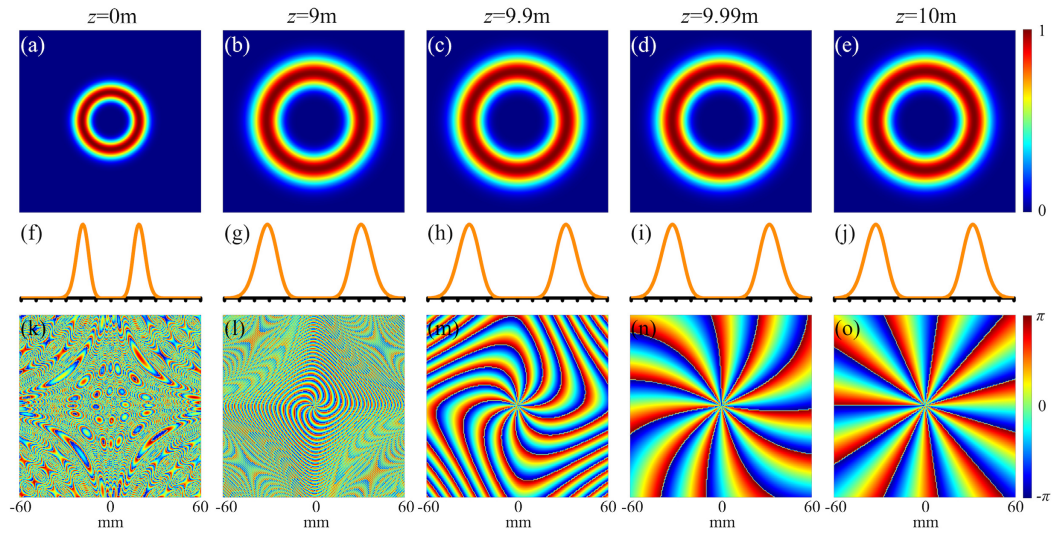

Fig. 3. Intensity profile of: (a) $l = 11$, $z = 0$ m; (b) $l = 11$, $z = 9$ m; (c) $l = 11$, $z = 9.9$ m; (d) $l = 11$, $z = 9.99$ m; (e) $l = 11$, $z = 10$ m; cross-section intensity profile of: (f) $l = 11$, $z = 0$ m; (g) $l = 11$, $z = 9$ m; (h) $l = 11$, $z = 9.9$ m; (i) $l = 11$, $z = 9.99$ m; (j) $l = 11$, $z = 10$ m; phase profile of: (k) $l = 11$, $z = 0$ m; (l) $l = 11$, $z = 9$ m; (m) $l = 11$, $z = 9.9$ m; (n) $l = 11$, $z = 9.99$ m; (o) $l = 11$, $z = 10$ m.

authors modulated the LG beam at $z = 0$ m by applying the phase shown in Fig. 3(k). After 10 m of underwater transmission, the phase is as shown in Fig. 3(o), where the isophase lines are straight and the OAM is clearly visible. Moreover, the compensation method proposed in this paper can also be applied to LG beams with higher or negative topological charges. This is significant for research on long-distance communication, imaging, and quantum sensing using LG beams.In this section, an underwater LG beam propagation simulation is performed and the phase twist is explored. Then, the authors conduct numerical calculations of underwater phase compensation and verify its correctness. After a long-distance underwater transmission, LG beams will diverge, and as the topological charge increases, the central dark region enlarges, and the phase becomes twisted. This is highly unfavourable for the distinction of OAM. This paper proposes a phase compensation method for LG beams in underwater transmission to address this issue. With this method, the phase is restored when the LG beam reaches the observation position after the underwater transmission and the isophase lines are straight, diverging outward along the optical axis. This has significant implications for research on vortex beams in cutting-edge fields such as communication, imaging, and quantum sensing.

4. Conclusions

LG beam is a type of vortex beam with a helical phase distribution. As the transmission distance increases, the phase distribution becomes twisted. Since the refractive index of water is higher than 1, this twist phenomenon is more severe in water. When the transmission distance is long and the topological charge is large, the phase becomes deformed, making the OAM indistinguishable, which hinders an advanced physical research. To solve this issue, this paper proposes a method for compensating the phase twist and studying the transmission characteristics of LG beams in water. Based on the physical principles of LG beams, using the initial light field and diffraction integral, the expression for the LG beam transmission in water is derived, isolating the exponential term responsible for the phase twist. Phase modulation is then applied to the initial LG beam. Through simulation, the proposed underwater LG beam phase compensation method ensures that, after underwater transmission, the isophase lines remain straight, greatly aiding in the accurate estimation of OAM and confirming the effectiveness of this method. The method proposed in this paper can be applied to LG beams with higher or negative topological charges. Theoretically, this paper proposes LG beams underwater transmission characteristics and phase compensation methods, offering potential value for LG beams and other vortex beams in fields such as underwater communication, imaging, and quantum sensing.

Authors' statement

Data analysis and interpretation, writing the article, H.S.; critical revision of the article, final approval of article, Y.W.; data analysis and interpretation, research concept and design, Y.Z.; collection and assembly of data, H.Q. & L.L.

Acknowledgements

This work was supported by the National Key R&D Program of China, National Quality Infrastructure (Grant no. 2021YFF0603800), National Natural Science Foundation of China (Grant no.1230030120), the Natural Science Foundation of Zhejiang Province (Grant no. LQ24A040005, LQ24F050006), and Cultivation Fund of Young Sci-tech Talents in CJLU (Grant no. 2023YW54, 2023YW62).

References

[1] Luski, A. *et al*. Vortex beams of atoms and molecules. *Science* **373**, 1105–1109 (2021). https://doi.org/10.1126/science.abj2451

[2] Mendoza-Hernández, J., Hidalgo-Aguirre, M., Inclán Ladino, A. & Lopez-Mago, D. Perfect Laguerre-Gauss beams. *Opt. Lett.* **45**, 5197–5200 (2020). https://doi.org/10.1364/OL.402083

[3] Pogrebnaya, A. O. & Rybas, A. F. Evolution of a circularly polarized beam bearing an optical vortex with fractional topological charge in a uniaxial crystal. *J. Opt. Technol*. **83**, 586–589 (2016). https://doi.org/10.1364/JOT.83.000586

[4] Chen, L. *et al.* Generation and conversion of a dual-band Laguerre-Gaussian beam with different OAM based on a bilayer metasurface. *Opt. Mater. Express* **12**, 1163–1173 (2022). https://doi.org/10.1364/OME.454031

[5] Li, Y.-L. & Luk, K.-M. A low-divergence circularly polarized dual-mode OAM antenna based on higher order Laguerre-Gaussian modes. *IEEE Trans. Antennas Propag.* **69**, 5215–5223 (2021). https://doi.org/10.1109/TAP.2021.3060028

[6] Wang, M. *et al.* Laguerre-Gaussian beam generation via enhanced intracavity spherical aberration. *Opt. Express* **29**, 27783–27790 (2021). https://doi.org/10.1364/OE.436110

[7] Yang, Y., Li, Y. & Wang, C. Generation and expansion of Laguerre–Gaussian beams. *J. Opt.* **51**, 910–926 (2022). https://doi.org/10.1007/s12596-022-00857-5

[8] Cui, Z., Hui, Y., Ma, W., Zhao, W. & Han, Y. Dynamical characteristics of Laguerre-Gaussian vortex beams upon reflection and refraction. *J. Opt. Soc. Am. B* **37**, 3730–3740 (2020). https://doi.org/10.1364/JOSAB.405281

[9] Volyar, A., Abramochkin, E., Akimova, Ya. & Bretsko, M. Control of the orbital angular momentum via radial numbers of structured Laguerre-Gaussian beams. *Opt. Lett.* **47**, 2402–2405 (2022). https://doi.org/10.1364/OL.459404

[10] Shen, D., He, T., Yu, X. & Zhao, D. Mode conversion and transfer of orbital angular momentum between Hermite-Gaussian and Laguerre-Gaussian beams. *IEEE Photonics J.* **14**, 1–6 (2022). https://doi.org/10.1109/JPHOT.2022.3140359

[11] Lian, Y. *et al*. OAM beam generation in space and its applications: A review. *Opt. Lasers Eng.* **151**, 106923 (2022). https://doi.org/10.1016/j.optlaseng.2021.106923

[12] Xia, T. *et al*. Properties of partially coherent elegant Laguerre-Gaussian beam in free space and oceanic turbulence. *Optik* 201, 163514 (2020). https://doi.org/10.1016/j.ijleo.2019.163514

[13] Li, Y., Cui, Z., Han, Y. & Hui, Y. Channel capacity of orbital-angular-momentum-based wireless communication systems with partially coherent elegant Laguerre-Gaussian beams in oceanic turbulence. *J. Opt. Soc. Am. A* **36**, 471 (2019). https://doi.org/10.1364/JOSAA.36.000471

[14] Yang, H., Yan, Q., Wang, P., Hu, L. & Zhang, Y. Bit-error rate and average capacity of an absorbent and turbulent underwater wireless communication link with perfect Laguerre-Gauss beam. *Opt. Express* **30**, 9053–9064 (2022). https://doi.org/10.1364/OE.451981

[15] Zhang, W., Wang, L., Wang, W. & Zhao, S. Propagation property of Laguerre-Gaussian beams carrying fractional orbital angular momentum in an underwater channel. *OSA Contin.* **2**, 3281–3287 (2019). https://doi.org/10.1364/OSAC.2.003281

[16] Xu, Y., Xu, Q. & Liu, W. Effect of oceanic turbulence on the propagation behavior of a radially polarized Laguerre-Gaussian Schell-model vortex beam. *J. Opt. Soc. Am. A* **40**, 1895–1907 (2023). https://doi.org/10.1364/JOSAA.494951

[17] Sheppard, C. J. R. & Porras, M. A. Comparison between the Propagation properties of Bessel-Gauss and generalized Laguerre-Gauss beams. *Photonics* **10**, 1011 (2023). https://doi.org/10.3390/photonics10091011

[18] Cheng, M. *et al*. Propagation of an optical vortex carried by a partially coherent Laguerre-Gaussian beam in turbulent ocean. *Appl. Opt*. **55**, 4642–4648 (2016). https://doi.org/10.1364/AO.55.004642

[19] Guo, S. *et al*. Research on propagation characteristic of Laguerre-Gaussian vortex beams with far-field scattering electric Monte Carlo method. *Opt. Commun.* **531**, 129214 (2023). https://doi.org/10.1016/j.optcom.2022.129214

[20] Zhang, Y., Yan, Q., Yu, L. & Zhu, Y. Information capacity of turbulent and absorptive underwater wireless link with perfect Laguerre-Gaussian beam and pointing errors. *J. Mar. Sci. Eng*. **10**, 1957 (2022). https://doi.org/10.3390/jmse10121957

[21] Longman, A. & Fedosejevs, R. Optimal Laguerre-Gaussian modes for high-intensity optical vortices. *J. Opt. Soc. Am. A* **37**, 841–848 (2020). https://doi.org/10.1364/JOSAA.389031

[22] Ghaderi Goran Abad, M. & Mahmoudi, M. Laguerre-Gaussian modes generated vector beam via nonlinear magneto-optical rotation. *Sci. Rep*. **11**, 5972 (2021). https://doi.org/10.1038/s41598-021-85249-8

[23] Zeng, Z. & Zhao, D. Superposed Laguerre-Gaussian beams-based orbital angular momentum holography. *Laser Photonics Rev*. **18**, 2300965 (2024). https://doi.org/10.1002/lpor.202300965

[24] Lembessis, V. E. & Babiker, M. Mechanical effects on atoms interacting with highly twisted Laguerre-Gaussian light. P*hys. Rev. A* **94**, 043854 (2016). https://doi.org/10.1103/PhysRevA.94.043854

[25] Liu, Y., Lin, R., Wang, F., Cai, Y. & Yu, J. Propagation properties of Laguerre-Gaussian Schell-model beams with a twist phase. *J. Quant. Spectrosc. Radiat. Transf.* **264**, 107556 (2021). https://doi.org/10.1016/j.jqsrt.2021.107556

[26] Xia, Y. *et al*. Experimental synthesis and demonstration of the twisted Laguerre-Gaussian Schell-mode beam. *Photonics* **10**, 314 (2023). https://doi.org/10.3390/photonics10030314

[27] Xiong, H., Huang, Y.-M. & Wu, Y. Laguerre-Gaussian optical sum-sideband generation via orbital angular momentum exchange. *Phys. Rev. A* **103**, 043506 (2021). https://doi.org/10.1103/PhysRevA.103.043506

[28] Isakov, D. *et al*. Evaluation of the Laguerre-Gaussian mode purity produced by three-dimensional-printed microwave spiral phase plates. *R. Soc. Open Sci.* **7**, 200493 (2020). https://doi.org/10.1098/rsos.200493